

0-A079 414

ARMY ELECTRONICS RESEARCH AND DEVELOPMENT COMMAND FO--ETC F/6 20/2
SURFACE AND SHALLOW BULK ACOUSTIC WAVES PROPAGATING ON DOUBLY R--ETC(U)
NOV 79 A BALLATO, T LUKASZEK, K H YEN

UNCLASSIFIED

DELET-TR-79-23

NL

1 OF
ADA 07944

END
10/10
10/10
2-80
info



12
PMS

A handwritten signature in black ink, likely belonging to a high-ranking official or supervisor.

RESEARCH AND DEVELOPMENT TECHNICAL REPORT

DELET-TR-79-23

SURFACE AND SHALLOW BULK ACOUSTIC WAVES PROPAGATING
ON DOUBLY ROTATED QUARTZ SUBSTRATES

ADA 079414

Arthur Ballato
Theodore Lukaszek

ELECTRONICS TECHNOLOGY & DEVICES LABORATORY

K. H. Yen
R. S. Kagiwada

TRW DEFENSE AND SPACE SYSTEMS GROUP
Redondo Beach, CA 90278

November 1979

DISTRIBUTION STATEMENT

Approved for public release;
distribution unlimited.

DDC FILE COPY

ERADCOM

US ARMY ELECTRONICS RESEARCH & DEVELOPMENT COMMAND
FORT MONMOUTH, NEW JERSEY 07703

80 1 - 9 047

NOTICES

Disclaimers

The citation of trade names and names of manufacturers in this report is not to be construed as official Government indorsement or approval of commercial products or services referenced herein.

Disposition

Destroy this report when it is no longer needed. Do not return it to the originator.

UNCLASSIFIED

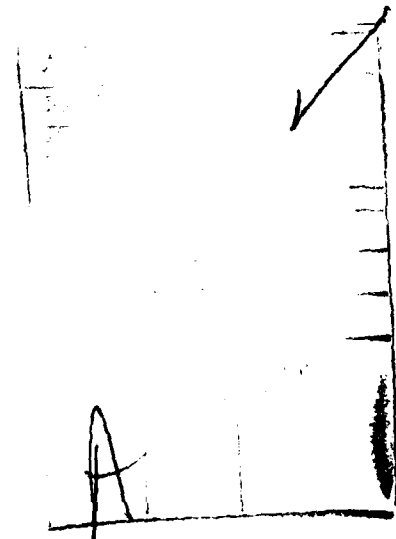
SECURITY CLASSIFICATION OF THIS PAGE (When Data Entered)

REPORT DOCUMENTATION PAGE		READ INSTRUCTIONS BEFORE COMPLETING FORM
1. REPORT NUMBER <i>(14)</i> DELET-TR-79-23	2. GOVT ACCESSION NO.	3. RECIPIENT'S CATALOG NUMBER
4. TITLE (and Subtitle) <i>(6)</i> Surface and Shallow Bulk Acoustic Waves Propagating on Doubly Rotated Quartz Substrates		5. TYPE OF REPORT & PERIOD COVERED <i>(9)</i> Technical Report
7. AUTHOR(s) <i>(10)</i> Arthur Ballato, Theodore Lukaszek, K.H. Yen, R.S. Kagiwada		6. PERFORMING ORG. REPORT NUMBER
9. PERFORMING ORGANIZATION NAME AND ADDRESS * US Army Electronics Technology & Devices Laboratory, (ERADCOM), Ft. Monmouth, NJ 07703 ATTN: DELET-MM		8. CONTRACT OR GRANT NUMBER(s)
11. CONTROLLING OFFICE NAME AND ADDRESS US Army Electronics Research & Development Command, Fort Monmouth, NJ 07703 ATTN: DELET-MM		10. PROGRAM ELEMENT, PROJECT, TASK AREA & WORK UNIT NUMBERS <i>(16)</i> 1L1 62705 AH94 09 011
14. MONITORING AGENCY NAME & ADDRESS (if different from Controlling Office) 9. Continued + TRW Defense and Space Systems Group Redondo Beach, CA 90278		12. REPORT DATE <i>(11)</i> NOVEMBER 1979
16. DISTRIBUTION STATEMENT (of this Report) Approved for Public release; distribution unlimited.		13. NUMBER OF PAGES 27
17. DISTRIBUTION STATEMENT (of the abstract entered in Block 20, if different from Report)		15. SECURITY CLASS. (of this report) UNCLASSIFIED
18. SUPPLEMENTARY NOTES		15a. DECLASSIFICATION/DOWNGRADING SCHEDULE <i>(12) 311</i>
19. KEY WORDS (Continue on reverse side if necessary and identify by block number) Crystal Resonators AT-cut Quartz Shallow Bulk Acoustic Waves Crystal Oscillators Quartz Crystals Bulk Acoustic Waves Piezoelectric Crystals Frequency Control Surface Acoustic Waves Piezoelectric Vibrators Frequency-Temperature Doubly Rotated Crystals Characteristics		
20. ABSTRACT (Continue on reverse side if necessary and identify by block number) ► Doubly rotated cut quartz possesses many desirable features for acoustic wave devices. In addition to its excellent temperature behavior, its nonlinear elasticity produces mechanical and thermal stress-compensating effects. Doubly rotated cuts of quartz have been extensively used to construct bulk wave resonators for frequency-stable sources. In this report we will describe the acoustic properties of Surface Acoustic Waves (SAW) and Shallow Bulk Acoustic Waves (SBAW) on doubly rotated quartz. A number of delay lines have been constructed on various doubly rotated cuts of quartz. The frequency		

UNCLASSIFIED

SECURITY CLASSIFICATION OF THIS PAGE(When Data Entered)

response of SAW is similar to that obtained on ST-cut quartz. The three SBAW modes predicted from theory were also observed. Both theoretical and experimental results are presented.



UNCLASSIFIED

SECURITY CLASSIFICATION OF THIS PAGE(When Data Entered)

CONTENTS

INTRODUCTION	1
SURFACE ACOUSTIC WAVES (SAW)	1
BULK ACOUSTIC WAVES (BAW)	3
SAW ON DOUBLY ROTATED CUT QUARTZ	3
SBAW ON DOUBLY ROTATED CUT QUARTZ	5
CONCLUSION	27

FIGURES:

1. Block Diagram of Measurement System	6
2. Frequency-Temperature Curve. ST Cut Quartz	8
3. Frequency-Temperature Curve. Unit 1-1-V	9
4. Frequency-Temperature Curve. Unit 1-1-0	10
5. Frequency-Temperature Curve. Unit 1-2-V	11
6. Frequency-Temperature Curve. Unit 2-1-V	12
7. Frequency-Temperature Curve. Unit 3-1-V	13
8. Frequency-Temperature Curve. Unit 3-1-0	14
9. Frequency-Temperature Curve. Unit 3-2-V	15
10. Frequency-Temperature Curve. Unit 4-1-V	16
11. Frequency-Temperature Curve. Unit 4-1-0	17
12. Frequency-Temperature Curve. Unit 4-2-V	18
13. Frequency-Temperature Curve. Unit 4-2-0	19
14. Frequency-Temperature Curves. Unit 5-1-V	20
15. Frequency-Temperature Characteristic	21
16. SAW Delay Line Response	21
17. SAW Velocity vs Angle psi	22
18. Calculated $\Delta v/v$ for SAW	22

19. Power Flow Angle vs psi	23
20. Comparison of BAW and SBAW Propagation	23
21. Temperature Coefficient Loci	25
22. SBAW Frequency Response	25
23. BAW Inverse Velocity Surface	26
24. BAW $\Delta v/v$ on Quartz	26
25. Power Flow Angle vs theta	27

TABLES:

1. Calculated and Measured Characteristics of SAW on Doubly Rotated Cut Quartz	4
2. X"-Propagating Surface Acoustic Waves on Doubly Rotated Quartz Substrates	7

INTRODUCTION

Doubly rotated cut quartz possesses many desirable features for acoustic wave devices. In addition to its excellent temperature behavior, its nonlinear elasticity produces mechanical and thermal stress-compensating effects. Doubly rotated cuts of quartz have been extensively used to construct bulk wave resonators for frequency-stable sources. In this paper we will report the acoustic properties of Surface Acoustic Waves (SAW) and Shallow Bulk Acoustic Waves (SBAW) on doubly rotated quartz.

A number of acoustic wave delay lines have been fabricated on doubly rotated cut quartz in the neighborhood of the zero temperature coefficient locus for bulk wave cuts. These delay lines consisted of two 4-finger per period transducers, each having 140 finger pairs. The finger widths were 2.361 micrometers. The delay lines were fabricated both along the X_1'' -axis direction and the normal to this direction. Surface acoustic waves propagate along the X_1'' -axis primarily, while shallow bulk acoustic waves propagate primarily normal to the X_1'' -axis.

The frequency response of SAW is similar to that obtained on ST-cut quartz, and the frequency-temperature behavior is likewise parabolic, with a somewhat improved second-order term. In general, the plates examined had high turn over temperatures, but optimum crystal orientations are not claimed. In addition, the three SBAW modes predicted from theory were also observed.

SURFACE ACOUSTIC WAVES (SAW)

The theory of surface waves in a piezoelectric substrate is based on the solution of the coupled acoustic and electrostatic equations subjected to the surface boundary condition. Inside the medium, the coupled equations under the quasi-static approximation for a piezoelectric medium may be written as

$$\left. \begin{aligned} \rho \ddot{u}_j - c_{ijkl} u_{k,il} - e_{ikl} \phi_{,ki} &= 0 \\ e_{ikl} u_{k,il} - \epsilon_{ik} \phi_{,ki} &= 0 \end{aligned} \right\} \quad (1)$$

and

where

ρ	= the mass density
u_i	= the mechanical displacement components
x_i	= the rectangular coordinates
c_{ijkl}	= the elastic tensor components
e_{ikl}	= the piezoelectric tensor components
ϵ_{ik}	= the dielectric permittivity tensor components
ϕ	= the scalar potential
$,k$	= $\partial/\partial x_k$; all subscripts take on the values 1,2, and 3.

1. A. Ballato, "Doubly Rotated Thickness Mode Plate Vibrators", in *Physical Acoustics: Principles and Methods*, (W.P. Mason and R.N. Thurston, eds.), Vol. 13, Chap. 5, Academic Press, New York, 1977, pp. 115-181.

Outside the piezoelectric medium, the potential satisfies Laplace's equation.

To solve for the surface wave, one lets

$$\left. \begin{aligned} u_j &= a_j e^{ik[\beta x_3'' + (1 + i\gamma)x_1'' - vt]} \\ \phi &= \alpha_4 e^{ik[\beta x_3'' + (1 + i\gamma)x_1'' - vt]} \end{aligned} \right\} \quad (2)$$

and

For surface acoustic waves, the attenuation constant γ is identically equal to zero.

Substituting Equation (2) into (1) yields

$$[A] [\alpha] = 0, \quad (3)$$

where $[A]$ is a 4×4 matrix and $[\alpha]$ is a 1×4 matrix. For a nontrivial solution of the components of $[\alpha]$, the determinant of the coefficient yields an eighth-order polynomial in β , of which four β roots are chosen.

The total solution for the allowable roots becomes

$$\left. \begin{aligned} u_j &= \sum_{n=1}^4 B(n) a_j^{(n)} e^{ik\beta(n)x_3'' e^{ik(x_1'' - vt)}} \\ \phi &= \sum_{n=1}^4 B(n) \alpha_4^{(n)} e^{ik\beta(n)x_3'' e^{ik(x_1'' - vt)}} \end{aligned} \right\} \quad (4)$$

and

$$\left. \begin{aligned} c_{3jk} u_{k,\ell} + e_{k3,j,k} &= 0 \\ -\epsilon_{3jk} \nabla \phi &= e_{3k\ell} u_{k,\ell} - e_{3k,j,k} = 0. \end{aligned} \right\} \quad (5)$$

The boundary conditions requiring that the stress vanishes and the normal component of electrical displacement is continuous at the surface ($x_3'' = 0$) may be written as

Substitution of the solutions given in (4) into (5) yields

$$[L] [B] = 0 \quad (6)$$

where $[L]$ is a 4×4 matrix and $[B]$ is a 1×4 matrix. Again, if the boundary conditions are to be satisfied by some combination of the $B^{(n)}$, the determinant of $[L]$ must vanish for an assumed value of v .

The method of solving for the surface acoustic wave is thus to assume a value of v , from Equation (3) obtain the corresponding values of γ 's and β 's and then check to see that it satisfies the boundary condition determinant $|L|$. If a value of v can be found which causes $|L|$ to vanish, then the surface wave exists and propagates at the velocity v .

BULK ACOUSTIC WAVES (BAW)

The theoretical description of the bulk acoustic wave is again obtained by solving the coupled acoustic and electrostatic equations. In contrast with the surface wave case, the boundary condition for the bulk wave case is that of an infinite medium. With this boundary condition, the form of the solution is a plane wave and can be written as

$$\left. \begin{aligned} u_j &= \beta_j e^{ik(x_j''-vt)} \\ \phi &= \beta_4 e^{ik(x_4''-vt)} \end{aligned} \right\} \quad (7)$$

where the unknowns are β_j and v .

Substituting these assumed solutions back into Equation (1) yields

$$[A'] [\beta'] = 0 , \quad (8)$$

where $[A']$ is a 4×4 matrix and $[\beta']$ a 1×4 matrix. For a non-trivial solution of the β 's to exist, the determinant of $[A']$ must be zero. This yields a sixth order polynominal in v , which can then be solved for the three (in general) positive and real velocities v_j . With v determined, one then can determine the β_j 's associated with each of the v_j 's. Each v_j is associated with a particular bulk acoustic wave mode such as longitudinal and transverse modes. Furthermore, the wave which propagates with a shallow angle from input transducer to output transducer is called a shallow-bulk acoustic wave.

SAW ON DOUBLY ROTATED CUT QUARTZ

The characteristics of SAW on doubly rotated quartz were theoretically calculated and experimentally measured on a number of non-optimal doubly rotated orientations. They are summarized in Table 1.

The theoretical calculation consists of first evaluation of the piezoelectric, elastic and dielectric constants at the desired crystal orientation. These material constants and their temperature coefficients have been well documented.² The SAW characteristics were then calculated using the theory discussed previously. For temperature coefficient of delay, the calculation further consists of computing the frequency of a SAW oscillator (which is directly obtained from oscillator phase condition) at different temperatures. By polynomial regression, the first and second order temperature coefficient of delay can be obtained with good accuracy.³

2. R. Bechmann, A.D. Ballato and T.J. Lukaszek, "Higher-Order Temperature Coefficients of the Elastic Stiffnesses and Compliances of Alpha-Quartz", Proceedings of the IRE, Vol. 50, No. 8, August 1962, pp. 1812-1822.

3. D. Hauden, M. Michel and J.J. Gagnepain, "Higher Order Temperature Coefficients of Quartz SAW Oscillators", Proceedings of the 32nd Annual Symposium on Frequency Control, 1978, US Army Electronics R&D Command, Fort Monmouth, NJ 07703, pp. 77-86.

Table 1. Calculated and Measured Characteristics
of SAW on Doubly Rotated Cut Quartz

Sample Group	Rotation Angles (degrees)	Turn-Over Temperature T_M (°C)	Coefficient of Delay		Piezoelectric Coupling k_2^2 (%)	Velocity v (cal) (km/sec)	Power Flow Angle (degrees)
			First Order $(10^{-6}/K)$	Second Order $(10^{-6}/K^2)$			
1	$\phi = 15$ $\theta = 34.3$	130 (meas) 130 (cal)	0	-28 -35	.14	3.2	-1.68
2	$\phi = 20$ $\theta = 34.7$	173 175	0	-20 -40	.15	3.24	-1.94
3	$\phi = 10$ $\theta = 34.8$	100 100	0	-18 -34	.13	3.175	-1.4
4	$\phi = 12$ $\theta = 34.8$	120 110	0	-28 -34	.135	3.18	-1.57
5	$\phi = 15$ $\theta = 34.8$	100 —	0	-30 —	.14	3.2	-1.82

To verify the theoretical calculations, temperature dependence measurements were made on all samples shown in Table 1, using the SAW oscillator configuration. The experimental setup consists of a SAW delay line as a feedback loop element around an HP8447 E amplifier. Because SAW delay lines have insertion loss less than 25 dB, no tuning circuit was used for the measurement. This eliminates the error introduced by the temperature dependence of the matching network.

Measurements were also made using a passive transmission system, as shown in Figure 1. A comparison is given in Table 2 of results obtained by both oscillator and passive (voltmeter) methods, on crystals different from those in Table 1, but belonging to the same groups. Devices are labeled as follows: the first number is the group number, second is the substrate number within the group, and third is the symbol "0" (oscillator measurement), or "V" (voltmeter measurement). Device 5-1-V was measured at three levels of five: 0.1, 0.4, and 0.8 volts; Table 2 shows that this device appeared to have the second order temperature coefficient of frequency modified by the drive level; the causes of this effect are at present unknown.

Figure 2 shows the frequency-temperature behavior of ST-cut quartz; the doubly rotated cuts to be described in the sequel are to be compared with this "standard" SAW characteristic. Figures 3 to 14 are frequency-temperature plots of doubly rotated quartz corresponding to the entries in Table 2.

Figure 15 shows the comparison of measured and theoretically calculated frequency temperature dependence for a sample from group 3. As shown in Figure 15, although the turn-around temperature agrees very well, the measured values have a smaller second-order coefficient of delay.

The frequency response of a SAW delay line on a sample from group 3 of Table 1 is shown in Figure 16. The measured untuned insertion loss is about 24 dB; propagation is along the X_1'' axis.

The theoretically calculated SAW velocity and $\Delta v/v$ of a sample from group 3 as a function of propagation angle ψ are shown in Figures 17 and 18, respectively. At the direction normal to the X_1'' -axis, $\Delta v/v$ is small. This is the direction used for SBAW application. The power flow angle as a function of ψ is shown in Figure 19. The power flow angle for SAW along the X_1'' -axis is about 1.4 degrees because the X_1'' -axis is not a pure mode axis for SAW propagation on doubly rotated cut quartz.

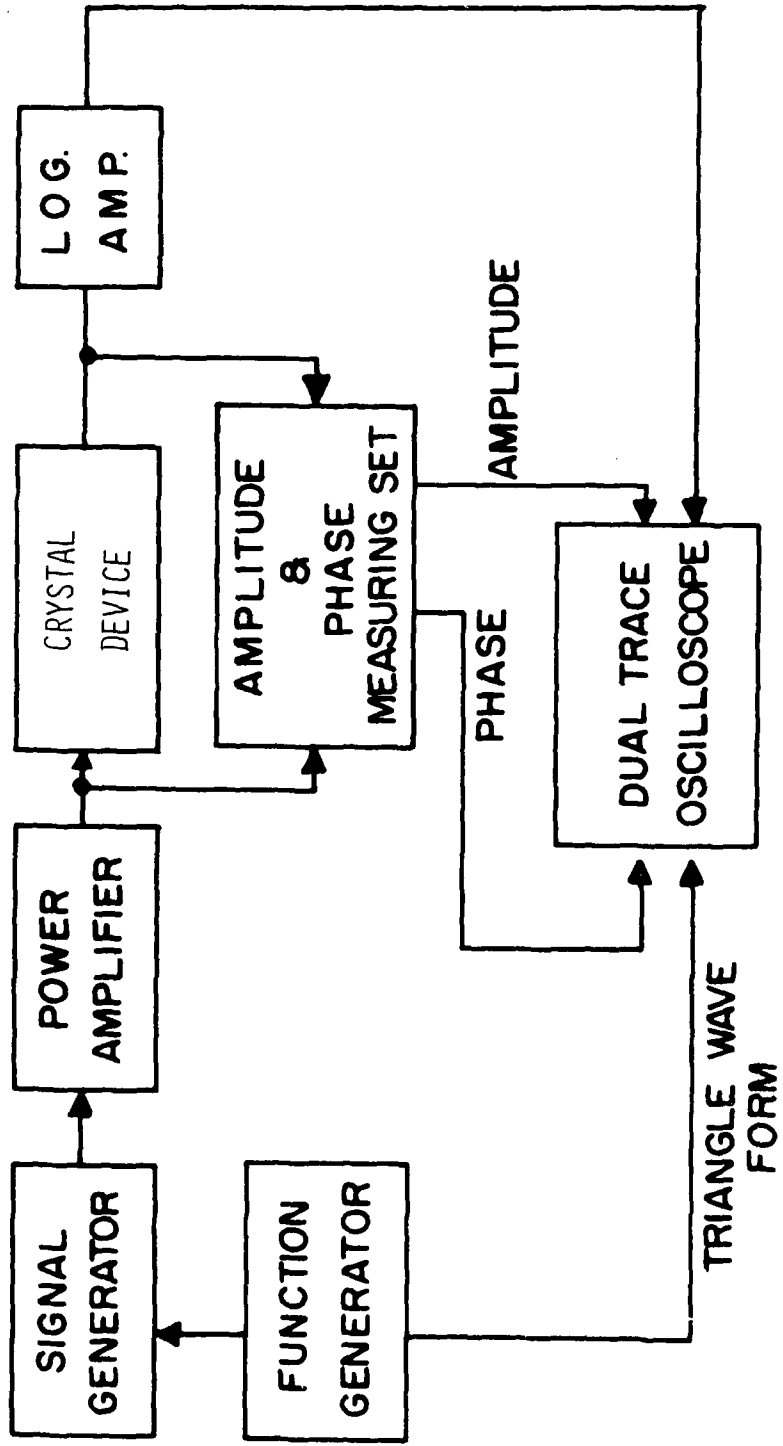
SBAW ON DOUBLY ROTATED CUT QUARTZ

Shallow bulk acoustic waves (SBAW) are shear horizontal waves which propagate just below the surface. SBAW devices have been configured into oscillators and filters using singly rotated quartz.^{4,5*} SBAW on doubly rotated cut quartz was first shown by Ballato and Lukaszek.^{6,7*} A list of SBAW references detailing work in this area is contained in Ref. 7; most of the advances have been due to the efforts of Lewis, and of Yen, Lau, and Kagiwada.

4. K.H. Yen, K.F. Lau, and R.S. Kagiwada, "Recent Advances in Shallow Bulk Acoustic Wave Devices," Proc. 1979 IEEE Ultrasonics Symposium, in press.

* Footnotes 5,6 and 7 are located on page 24.

PHASE & AMPLITUDE MEASUREMENTS



EQUIPMENT	DISPLAYS
PHASE & AMPLITUDE MEASURING SET	PHASE VS FREQUENCY AMPLITUDE VS PHASE
LOGARITHMIC AMPLIFIER	AMPLITUDE VS FREQUENCY

Figure 1. Block Diagram of Measurement System.

Table 2. X_1'' - Propagating Surface Acoustic Waves
on Doubly Rotated Quartz Substrates

Device	Orientation	Frequency (MHz)	T_μ (°C)	$T_f(1)$ ($\times 10^{-6}$)	$T_f(2)$ ($\times 10^{-9}$)	$(\Delta f/f)_\mu$ ($\times 10^{-6}$)
1-1-V	0 = 15°	169.105721	130.9	5.3	-25	281.0
1-1-0	0 = 34°18'	169.270860	128.7	5.6	-26.9	289.9
1-2-V		169.201921	160.9	7.0	-25.9	478.8
2-1-V	0 = 20°	171.153535	111.9	4.3	-24.9	188.4
2-2-V	0 = 34°40'	171.310797	450.5	11.8	-13.8	2504.
2-2-0		171.898107	326.4	12.6	-20.9	1899.
3-1-V	0 = 10°	167.415333	0.35	-1.0	-20.1	12.9
3-1-0	0 = 34°50'	167.566840	2.0	-1.2	-25.3	13.3
3-2-V		167.875497	125	4.3	-21.6	217.6
4-1-V	0 = 12°	168.031256	154	5.3	-20.3	340.4
4-1-0	0 = 34°46'	168.574371	156	6.1	-23.1	400.0
4-2-V		167.512109	113	4.6	-26.2	203.7
4-2-0		168.093820	104	3.5	-22.1	157.7
5-1-V1	0 = 15°	168.470556	95	7.3	-51	259.7
5-1-V4	0 = 34°46'	168.475937	97.5	4.9	-34	179.5
5-1-V8		168.494032	87.7	3.2	-26	102.1

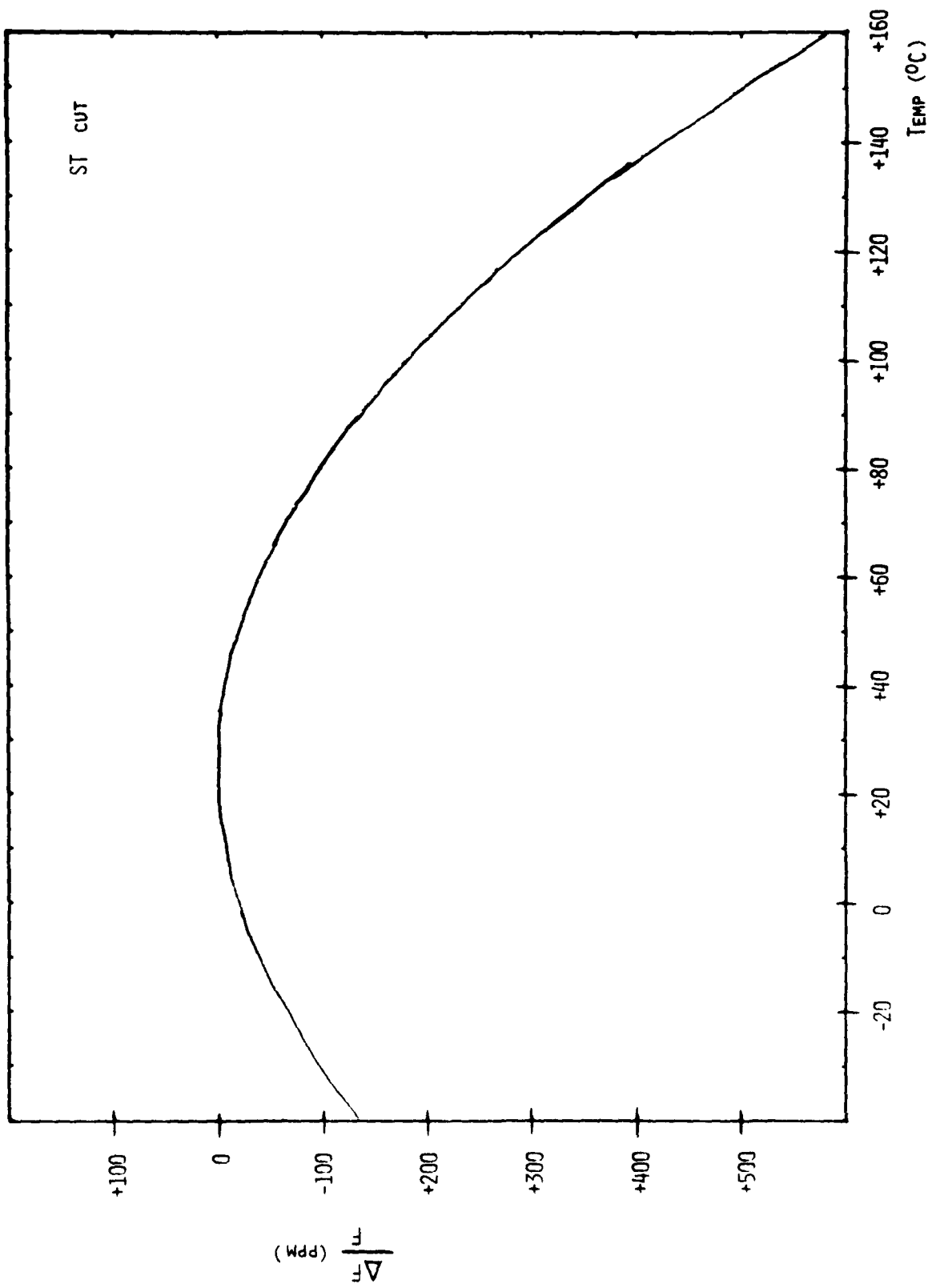


Figure 2. Frequency-Temperature Curve. ST Cut Quartz.

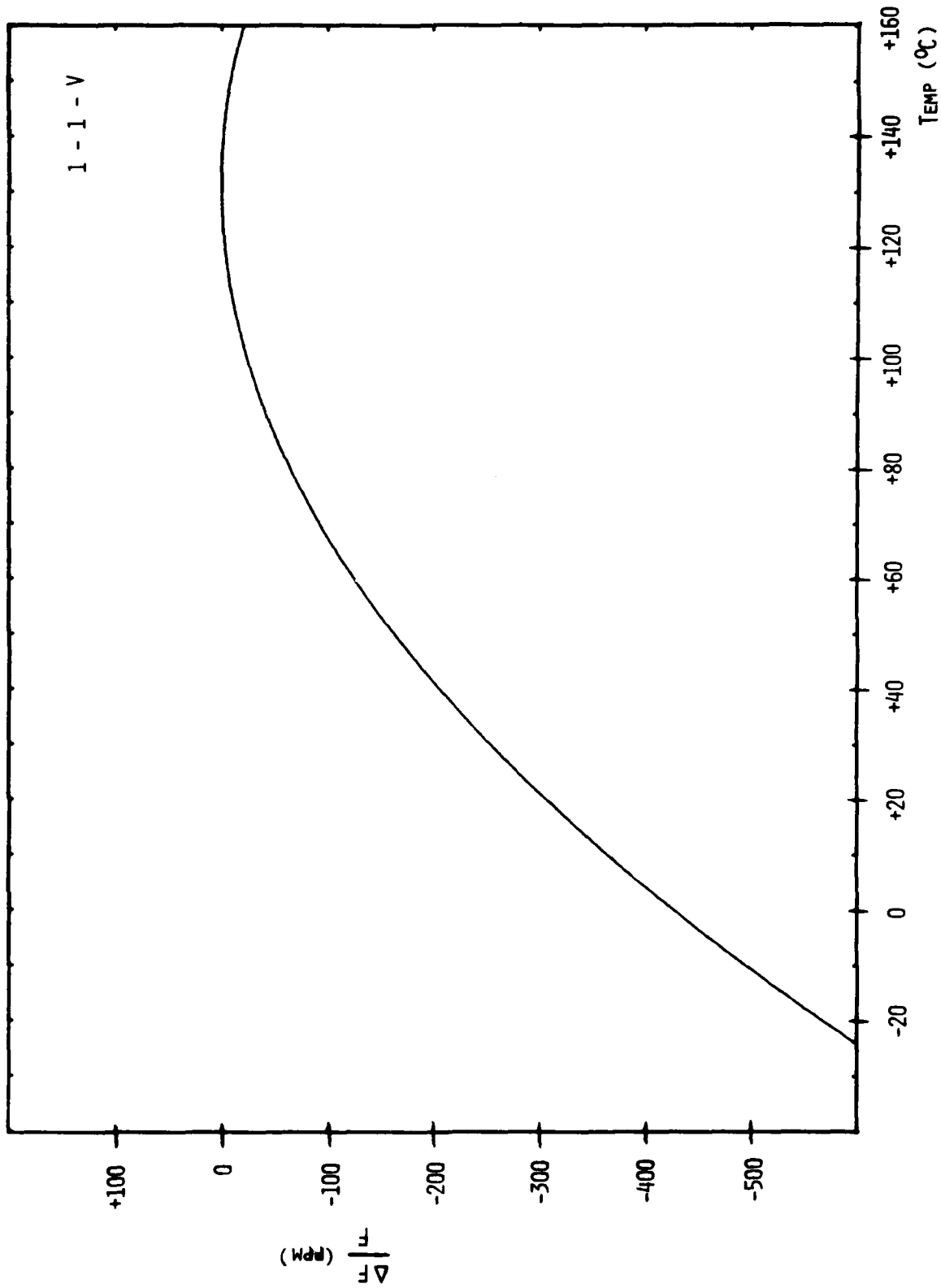


Figure 3. Frequency-Temperature Curve. Unit 1-1-V.

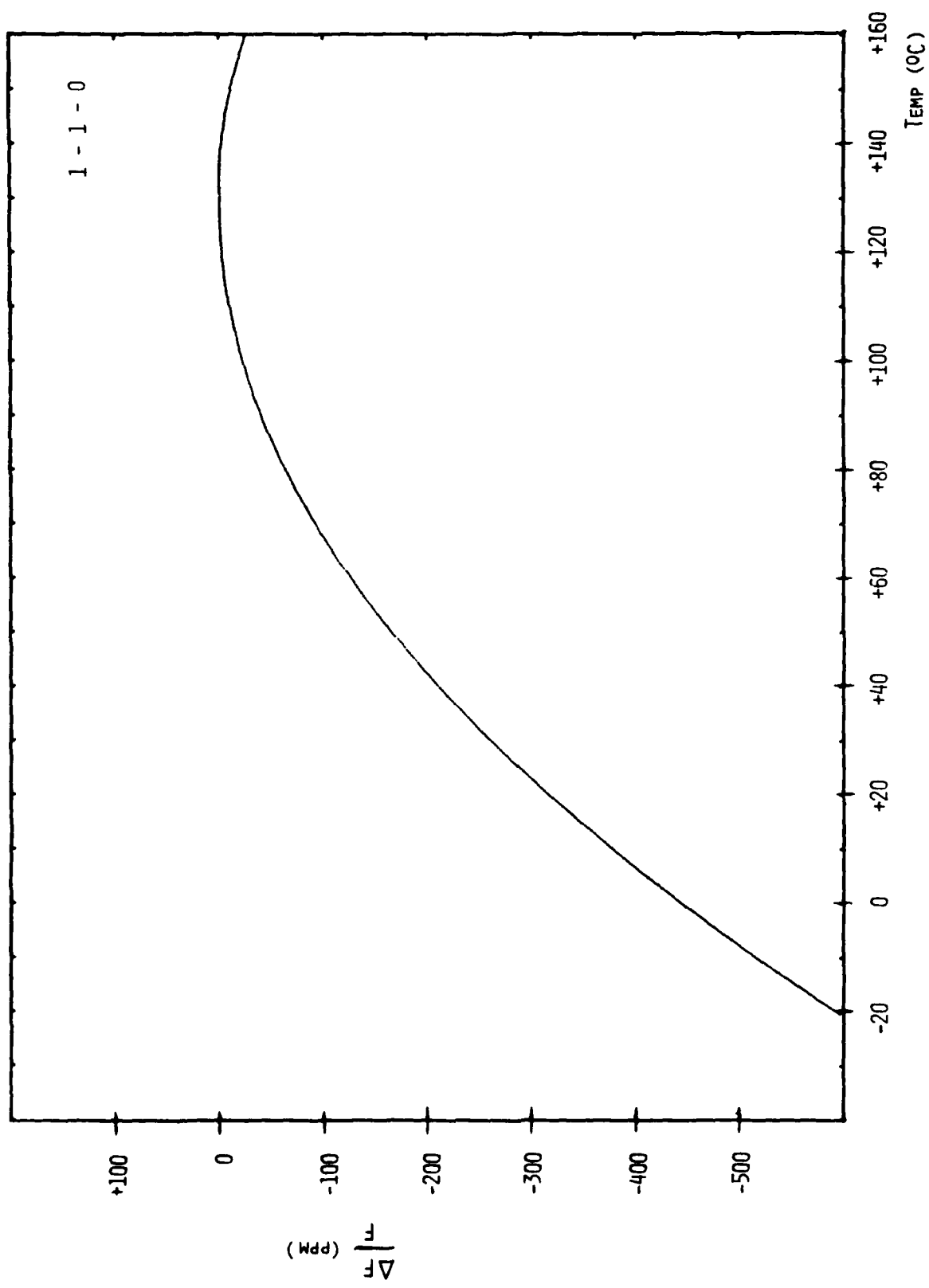


Figure 4. Frequency-Temperature Curve. Unit 1-1-0.

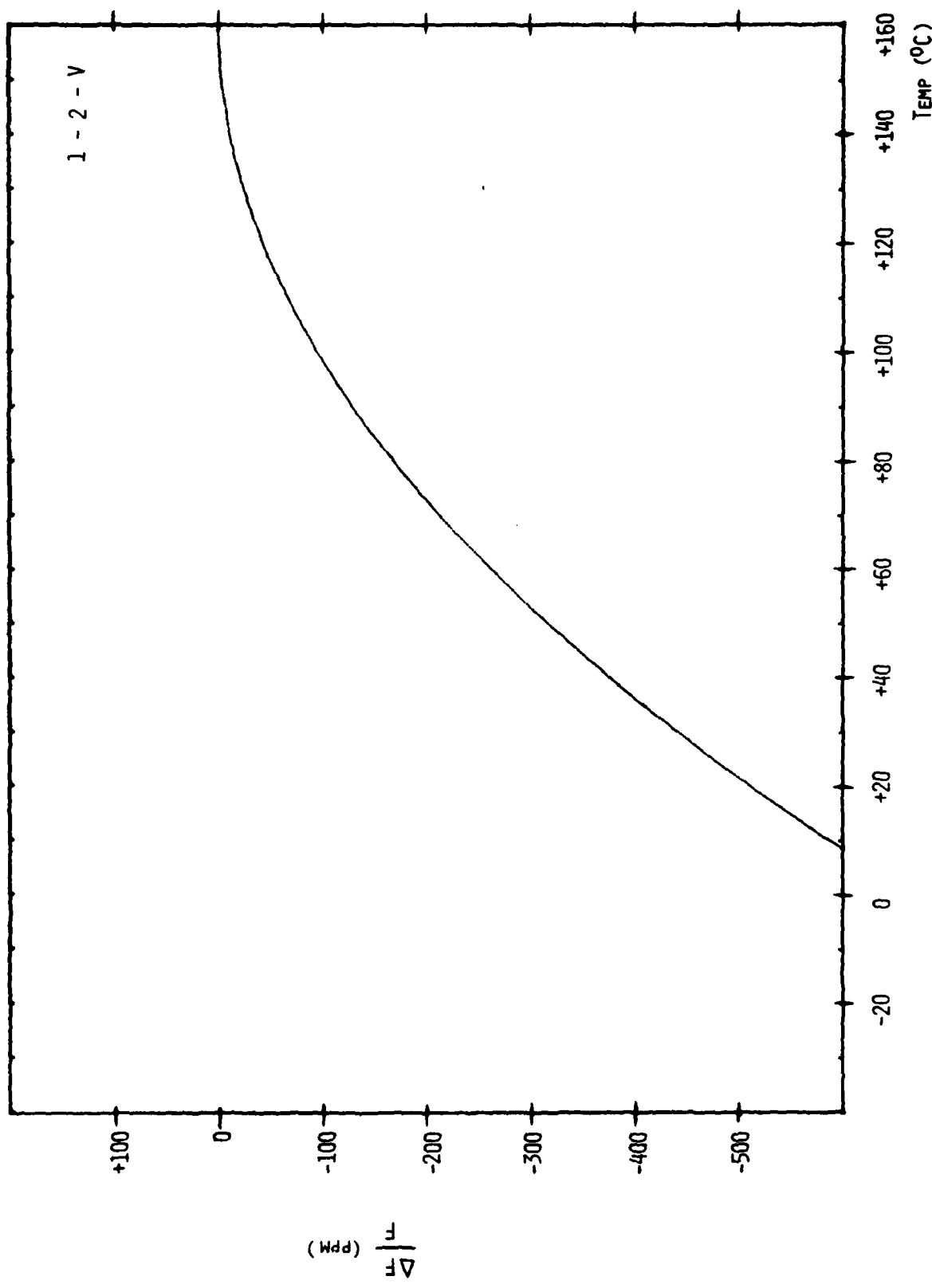


Figure 5. Frequency-Temperature Curve. Unit 1-2-V.

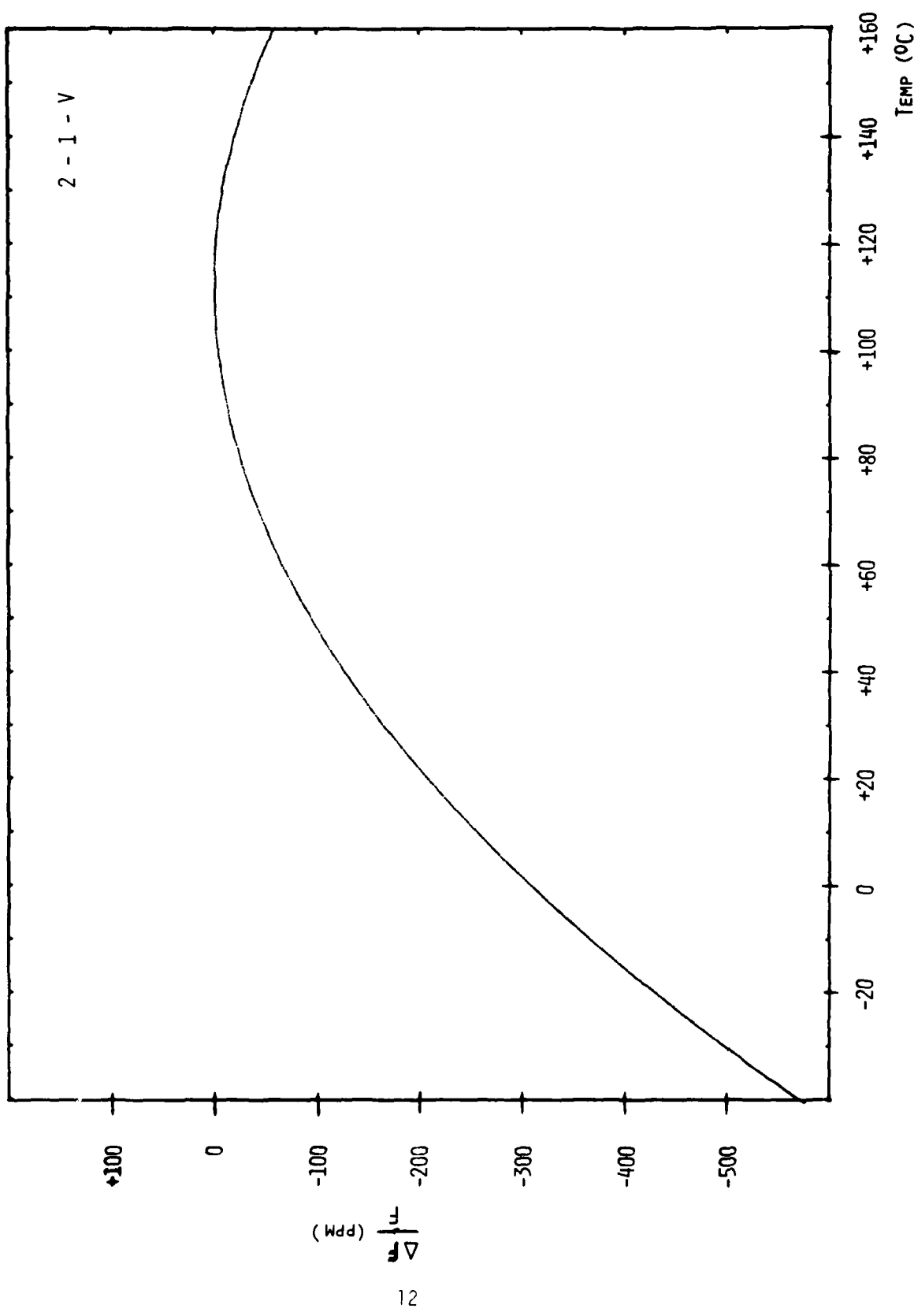


Figure 6. Frequency-Temperature Curve, Unit 2-1-V.

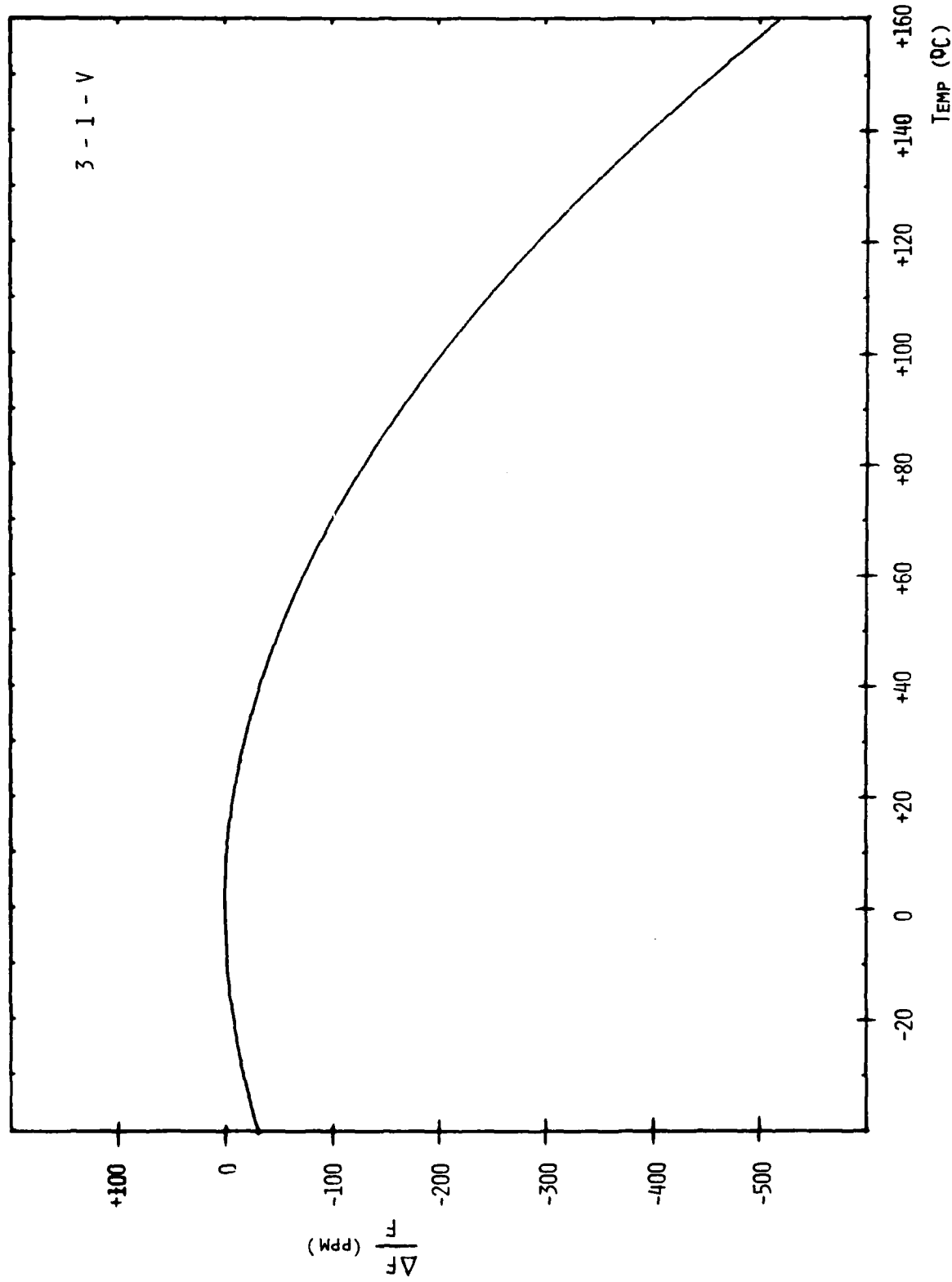


Figure 7. Frequency-Temperature Curve. Unit 3-1-V.

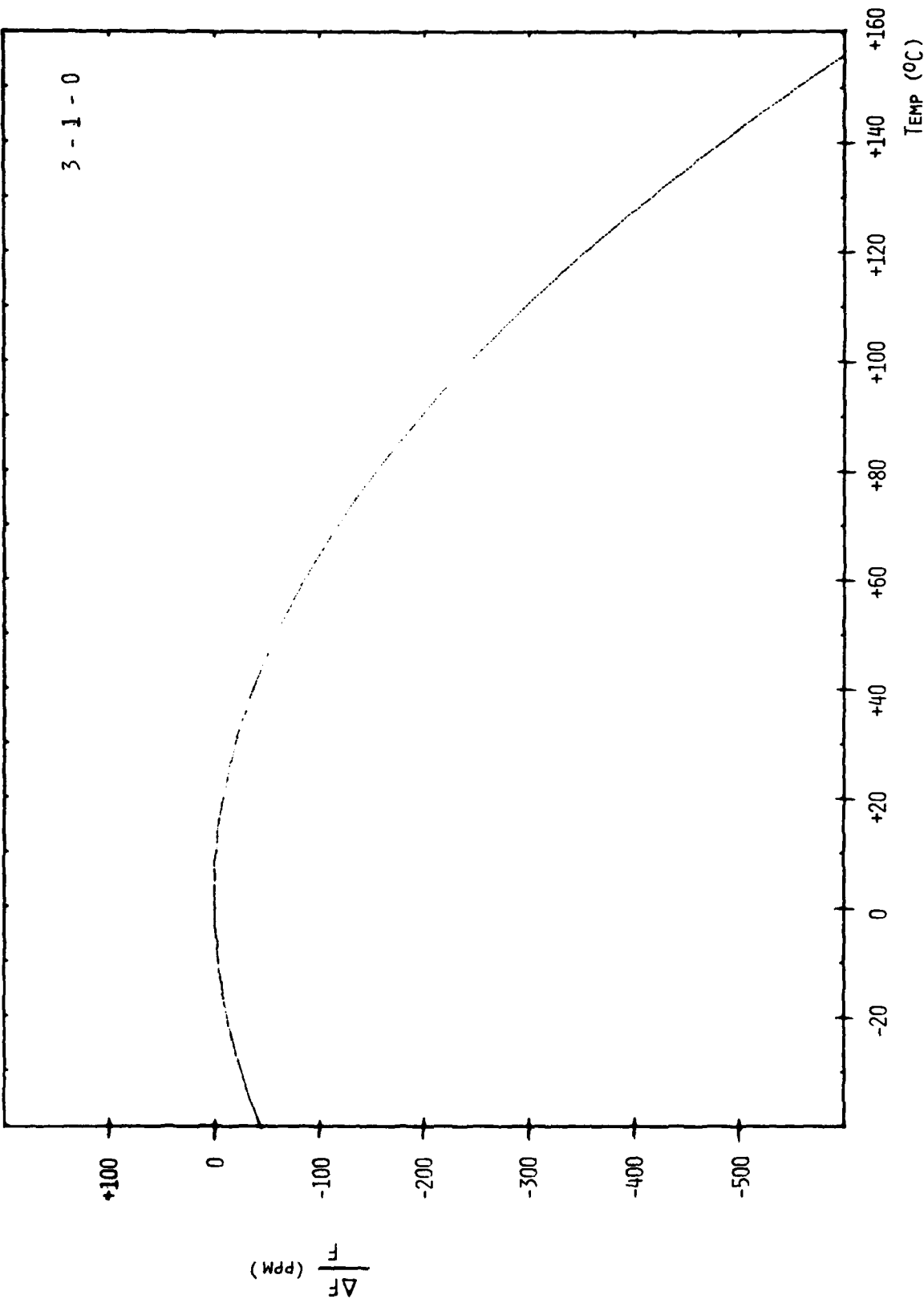


Figure 3. Frequency-Temperature Curve, Unit 3-1-0.

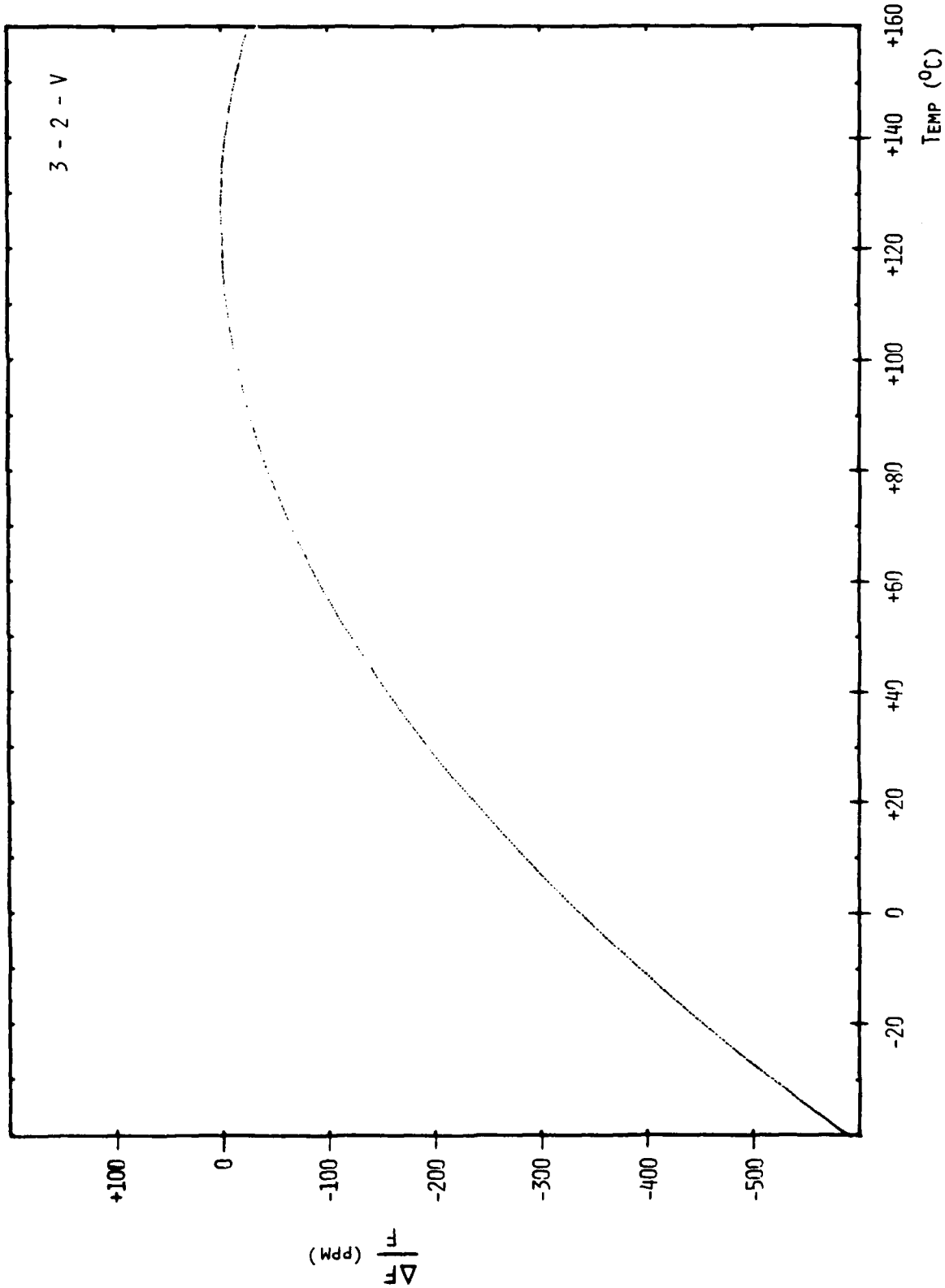
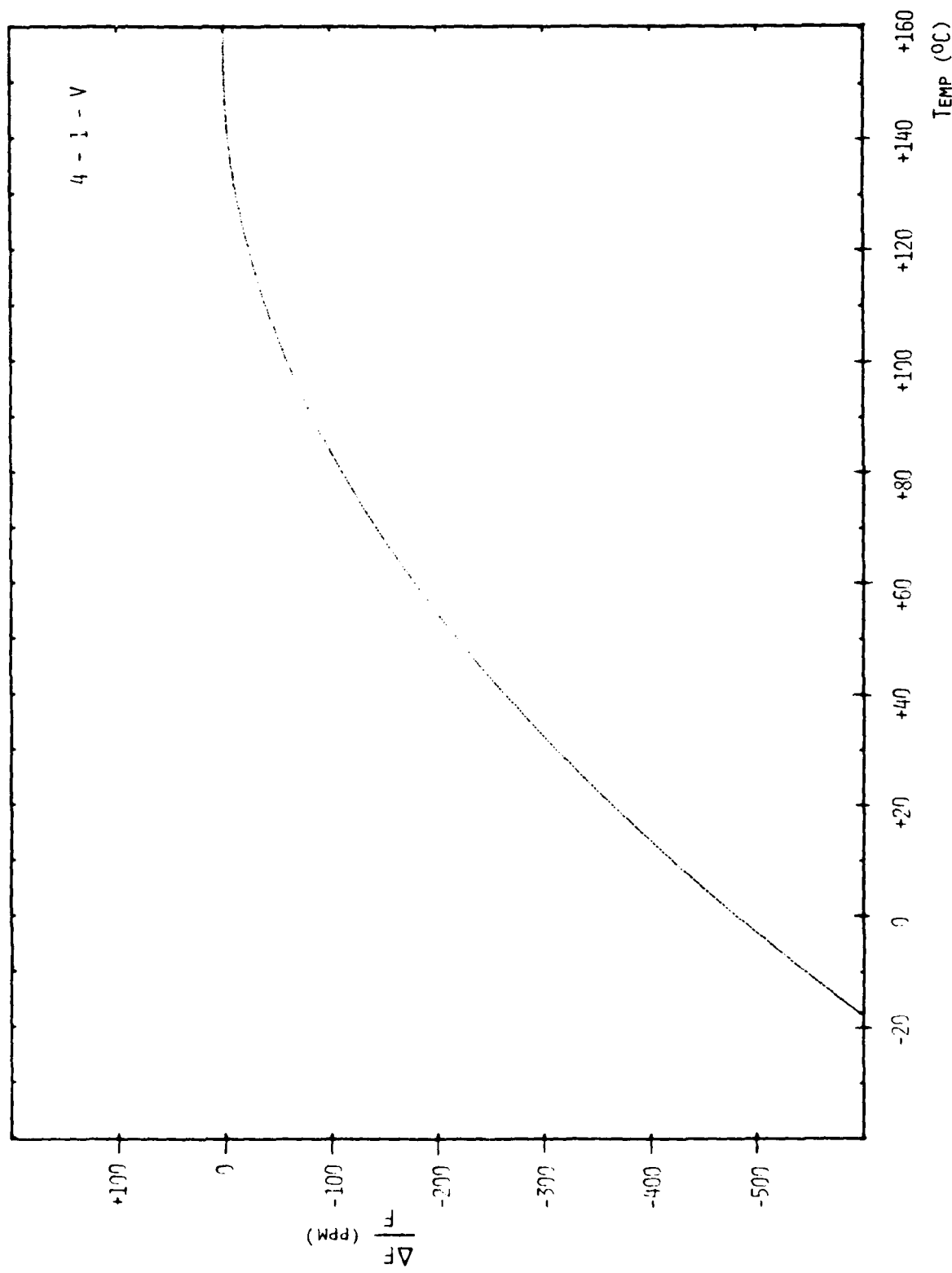


Figure 9. Frequency-Temperature Curve. Unit 3-2-V.

Fig. 10. Frequency-Temperature Curve. Unit: A-1-V.



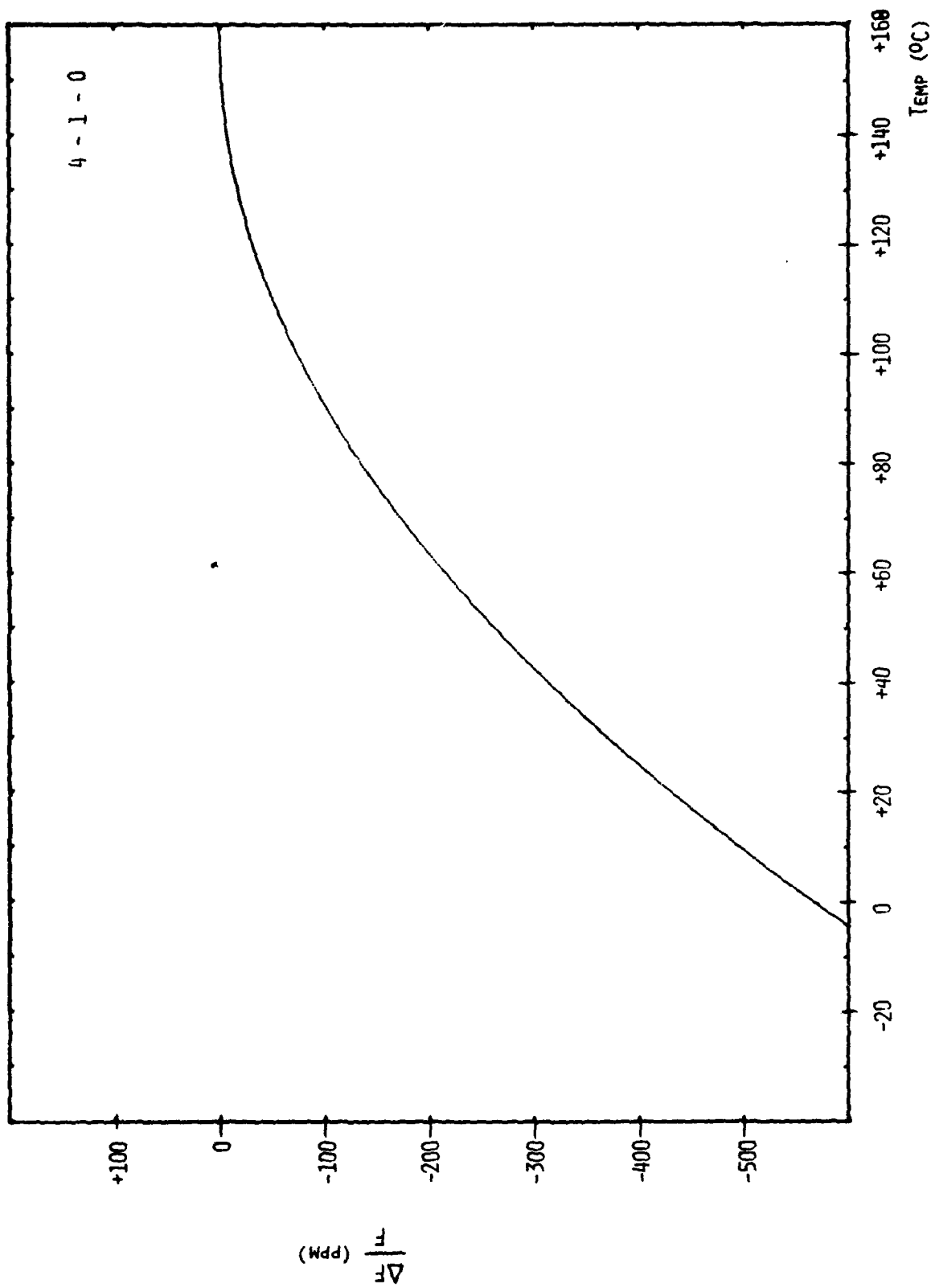


Figure 11. Frequency-Temperature Curve. Unit 4-1-0.

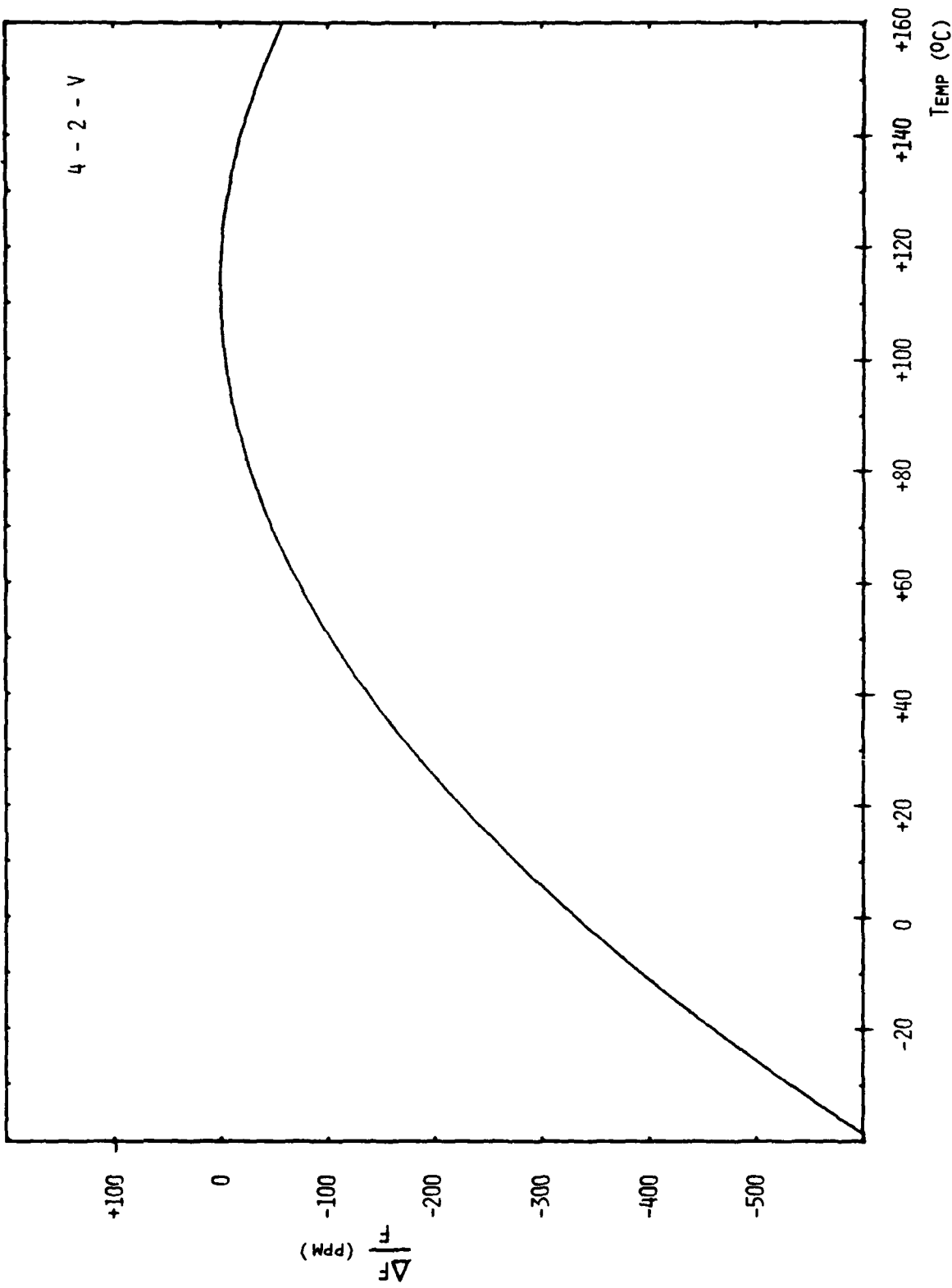


Figure 12. Frequency-Temperature Curve. Unit 4-2-V.

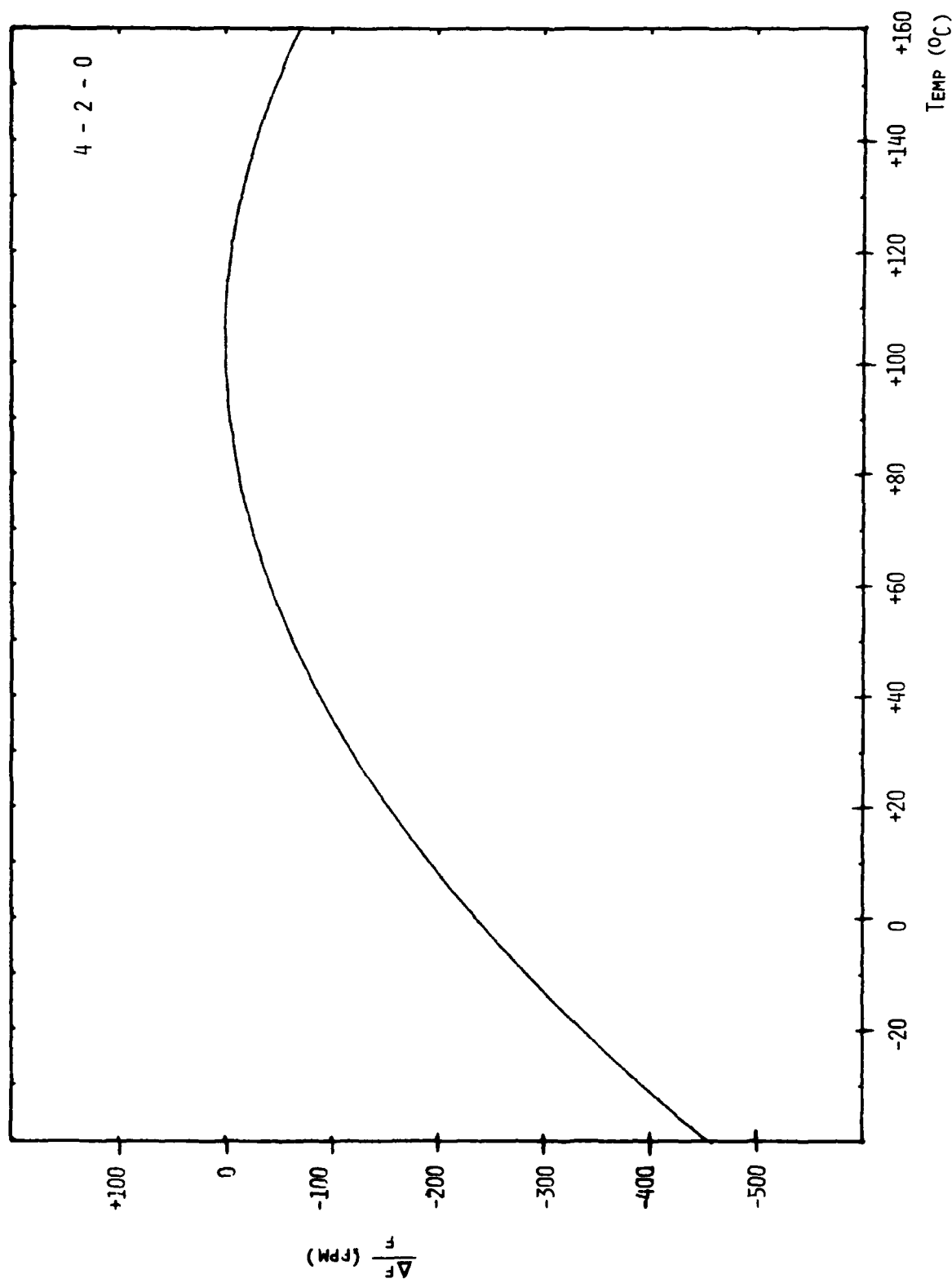


Figure 13. Frequency-Temperature Curve. Unit 4-2-0.

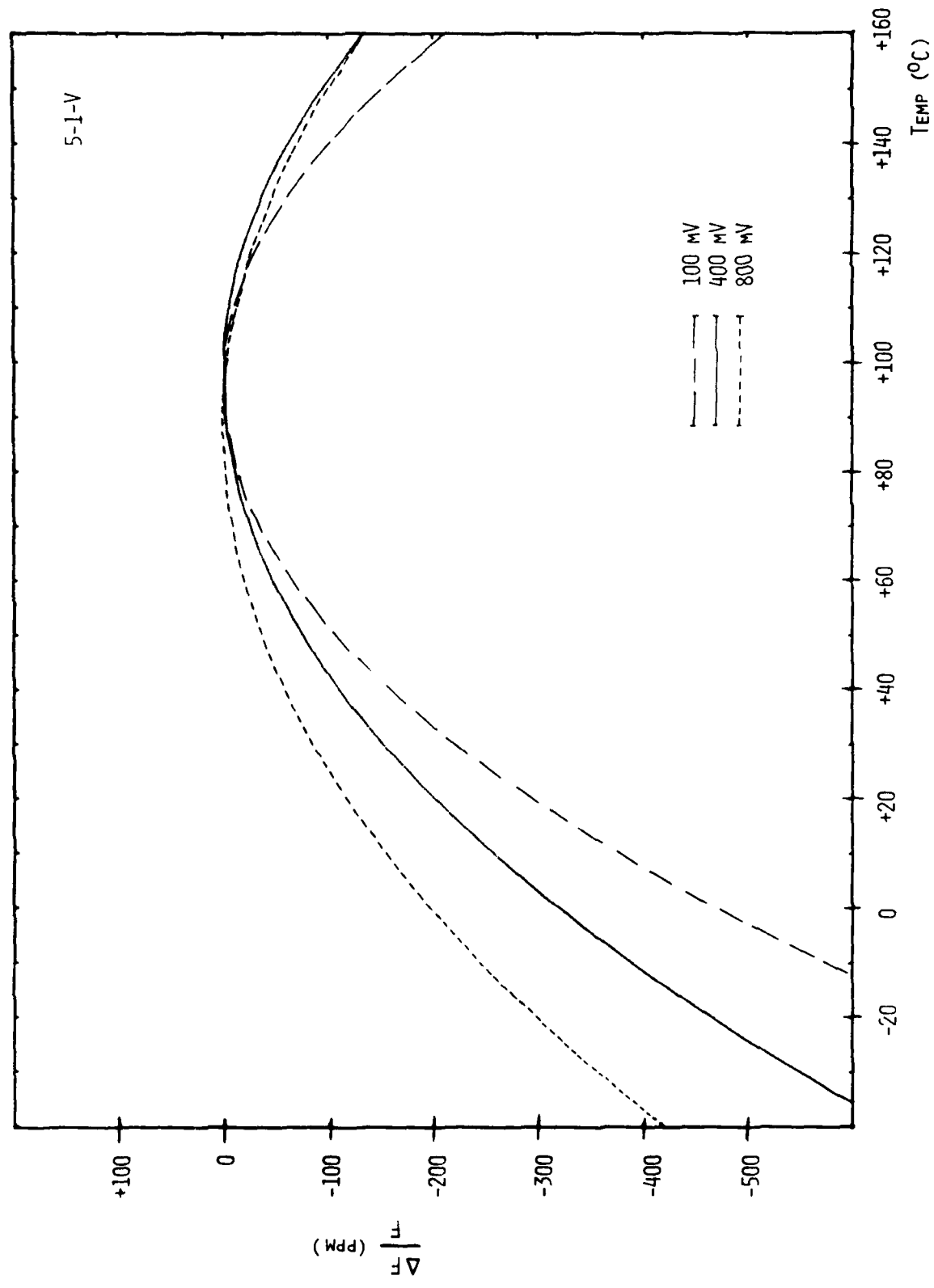


Figure 14. Frequency-Temperature Curves. Unit 5-1-V.

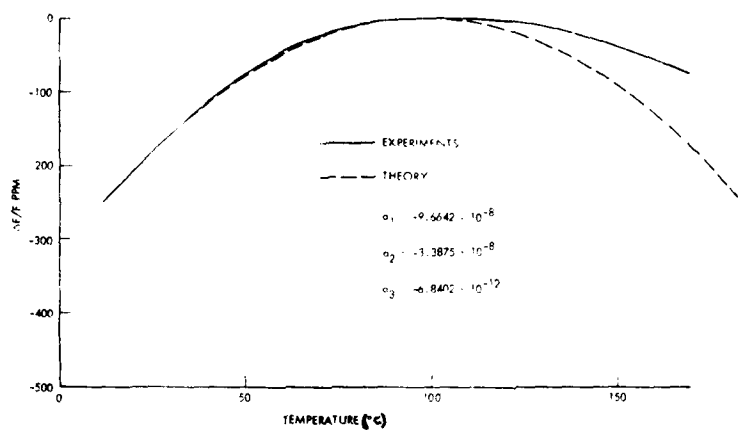


Figure 15. Frequency-Temperature Characteristic.

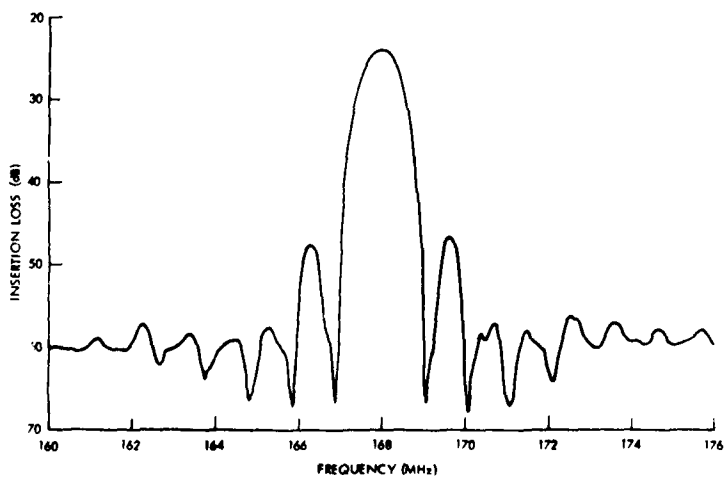


Figure 16. SAW Delay Line Response.

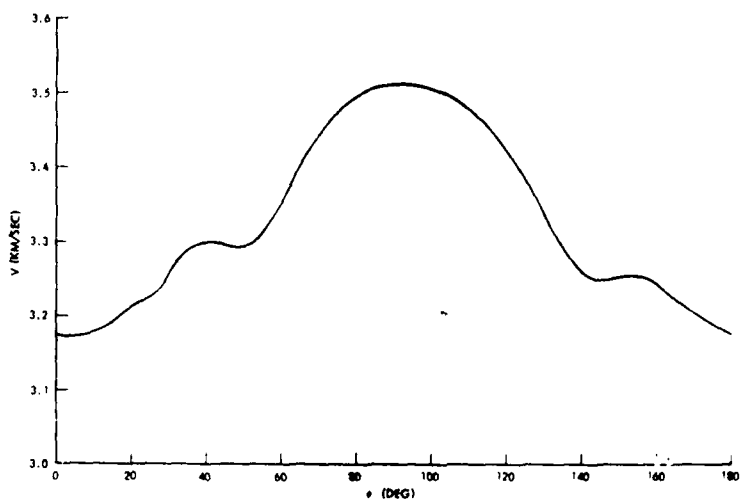


Figure 17. SAW Velocity vs Angle ψ .

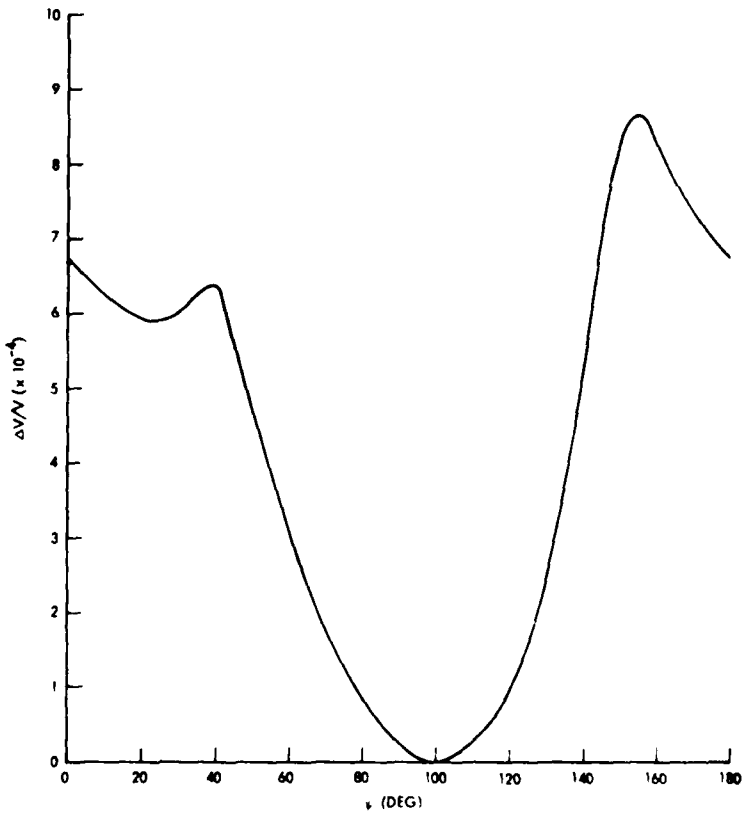


Figure 18. Calculated $\Delta v/v$ for SAW.

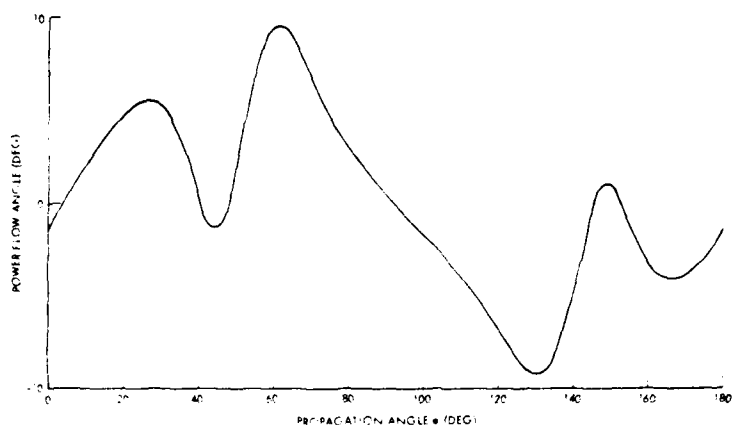


Figure 19. Power Flow Angle vs psi.

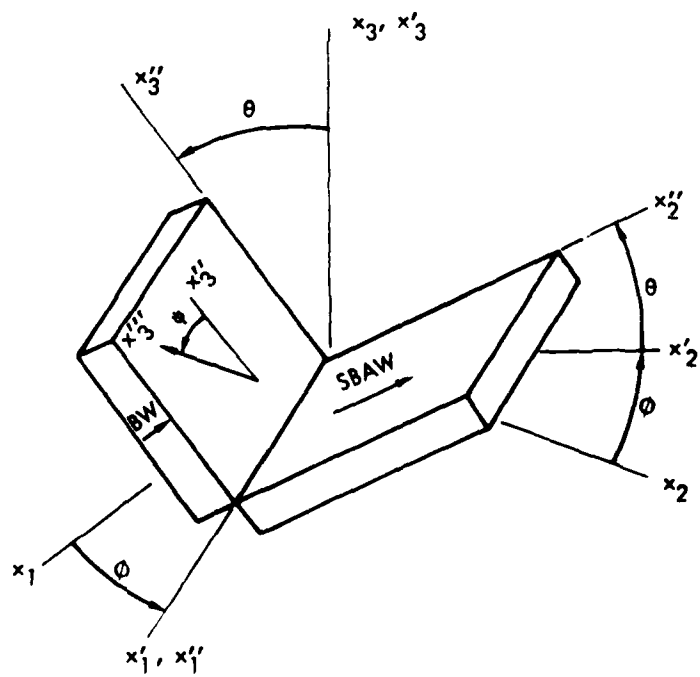


Figure 20. Comparison of BAW and SBAW Propagation.

The relationship between bulk wave and SBAW is shown in Figure 20. They are normal to each other. Figure 21 shows the relationship of bulk acoustic wave resonator and SBAW devices along the AT-cut zero temperature coefficient branch (line a) and the BT-cut branch (line b). For SBAW devices to have properties similar to bulk acoustic wave resonator along the AT-branch, one has to use substrates prepared approximately along line a'. Similar relationships hold for line b and line b'. (Also shown in Figure 21 is the zero temperature coefficient loci for SAW propagating along X'' -axis.) This BAW and SBAW relationship on doubly rotated cut quartz has been demonstrated.^{6,7}

Figure 22 shows the frequency response of the fast shear horizontal wave propagating along the direction normal to the X'' -axis. This bulk wave has been identified as a shallow bulk acoustic wave which propagates just below the surface from input transducer to output transducer. The measured un-tuned insertion loss was about 22 dB. The center frequency was about 1.4 times that of SAW's, which was at 185 MHz and was about 40 dB lower in amplitude than SBAW. The passband distortion is due to multiple reflections from the ends of the delay line.

The inverse velocity surface for doubly rotated cut quartz ($\phi = 10^0$; $\psi = 90^0$) is shown in Figure 23. The axis for a sample from group 3 is also shown in this figure along with the cutoff wave vector \bar{k}_c which corresponds to the ray (energy) directed parallel to the surface of the substrate. The calculated cutoff velocity for a sample from group 3 is about 4923 m/sec. The cutoff velocity determines the center frequency of operation of interdigital transducers. Thus, the calculated center frequency is 260.65 MHz which agrees very well with the measured value.

The calculated ($\Delta v/v$) for three bulk waves along the surface are shown in Figure 24. Although ($\Delta v/v$) is not the piezoelectric coupling constant needed in the equivalent circuit model, it indicates the relative coupling strength for each mode. As shown in Figure 24, for a sample from group 3, interdigital transducers can excite all three bulk waves. This has been shown by Ballato and Lukaszek.^{6,7} Figure 25 shows the power flow angle for fast shear waves in an infinite medium, where ϕ_{12} is the power steering angle on surface and ϕ_{13} is the beam steering angle into the substrate. The large values of ϕ_{12} and ϕ_{13} are due to the fact that waves propagating in doubly rotated cut quartz are not along the principal axis.

5. T.I. Browning and M.F. Lewis, "A Novel Technique for Improving the Temperature Stability of SAW/SSBW Devices", Proc. IEEE Ultrason. Symp., September 1978, pp. 474-477.

6. A. Ballato and T.J. Lukaszek, "Shallow Bulk Acoustic Wave Devices", 1979 MTT Digest, pp. 162-164. IEEE Catalog No. 79CH1439-9 MTT-S.

7. A. Ballato and T. Lukaszek, "Shallow Bulk Acoustic Waves-Progress and Prospects," IEEE Trans. Microwave Theory Tech., Vol. MTT-27, No. 12, December 1979, in press.

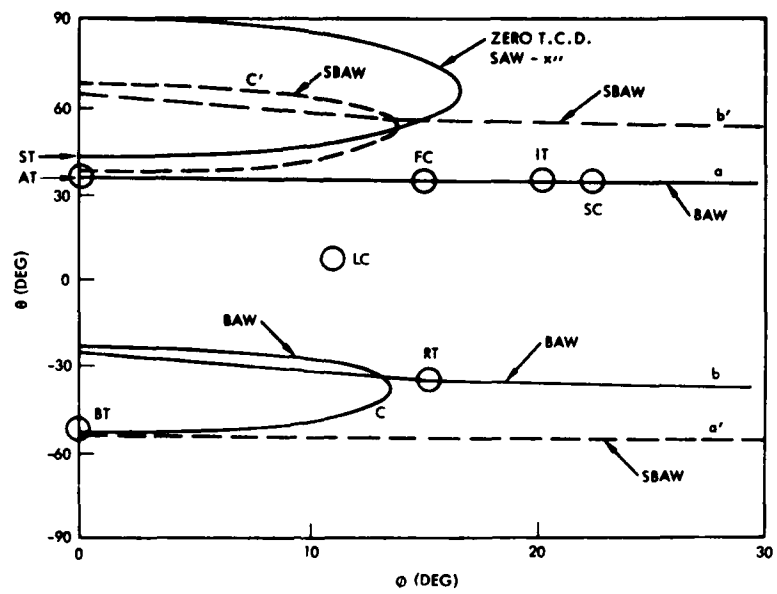


Figure 21. Temperature Coefficient Loci.

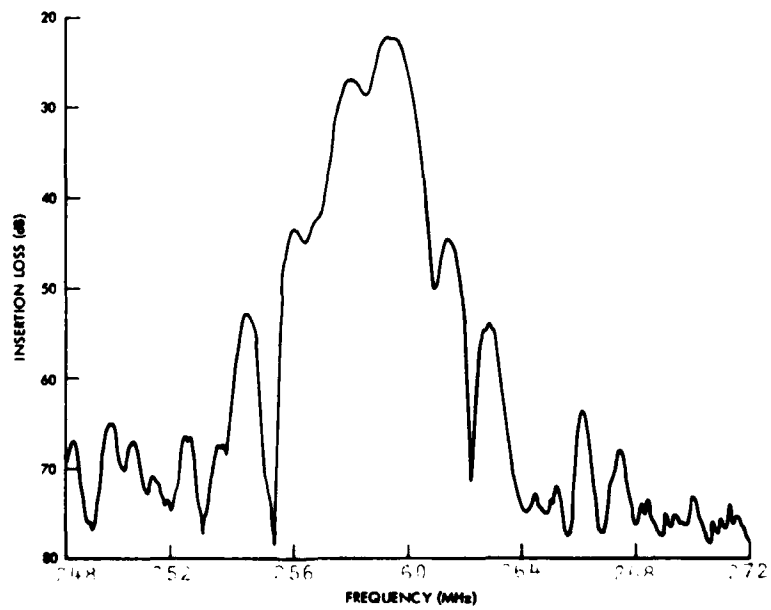


Figure 22. SBAW Frequency Response.

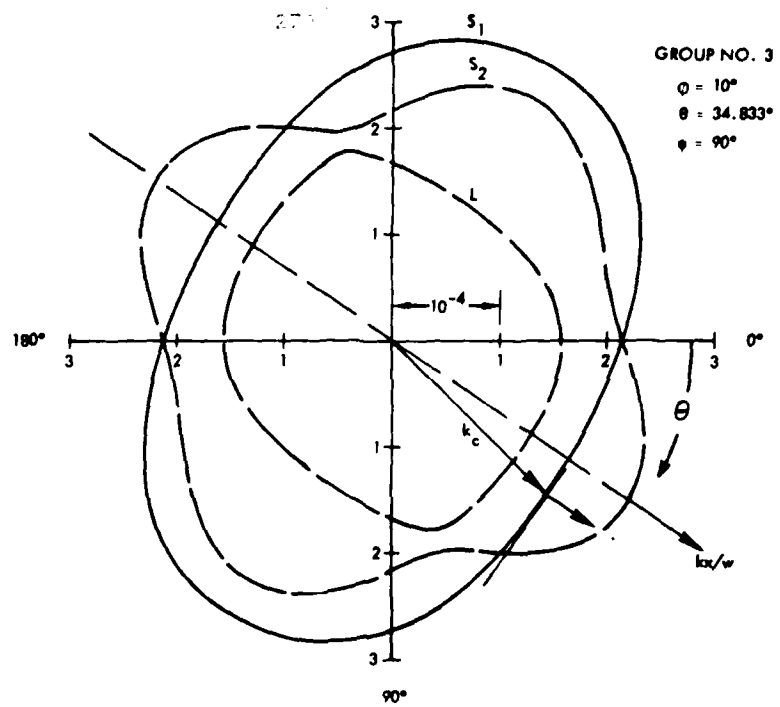


Figure 23. BAW Inverse Velocity Surface.

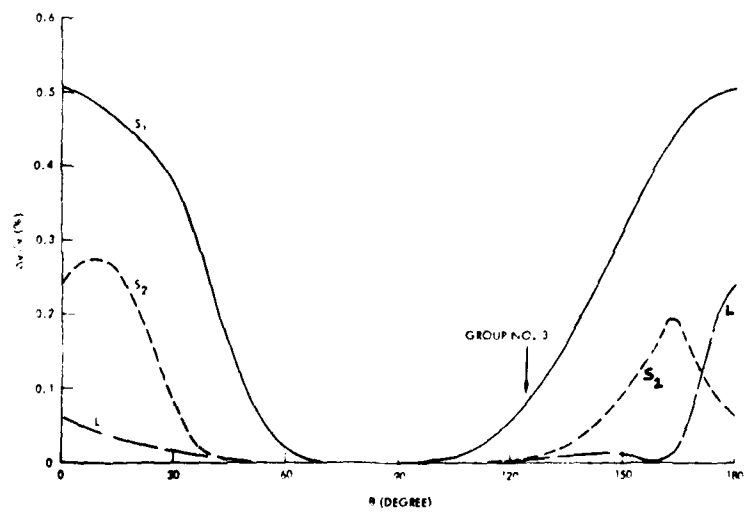


Figure 24. BAW $\Delta v/v$ on Quartz.

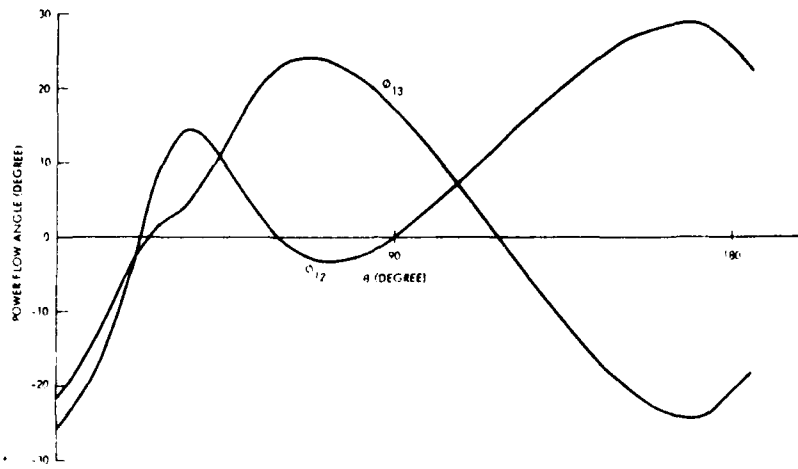


Figure 25. Power Flow Angle vs theta.

CONCLUSION

A number of delay lines have been constructed on various doubly rotated cuts. The frequency-temperature response of SAW is somewhat improved compared to that obtained on ST-cut quartz. Optimized orientations will lead to further improvements. In addition, the three SBAW modes predicted from theory were also observed. Because doubly rotated cut quartz possesses desirable temperature behavior and stress-compensating effects, it holds promise for construction of SAW and SBAW delay line oscillators with improved frequency-stable behavior.